Delft University of Technology

3D slope stability analysis with spatially variable and cross-correlated shear strength parameters

Varkey, Divya; Hicks, Michael; Vardon, Phil

Publication date
2018

Document Version
Accepted author manuscript

Published in
Proceedings of the 9th European Conference on Numerical Methods in Geotechnical Engineering (NUMGE 2018)

Citation (APA)
Varkey, D., Hicks, M., & Vardon, P. (2018). 3D slope stability analysis with spatially variable and cross-correlated shear strength parameters. In A. S. Cardoso, J. L. Borges, P. A. Costa, A. T. Gomes, J. C. Marques, & C. S. Vieira (Eds.), *Proceedings of the 9th European Conference on Numerical Methods in Geotechnical Engineering (NUMGE 2018)* (pp. 543-548). (Numerical Methods in Geotechnical Engineering; Vol. 9). CRC Press / Balkema - Taylor & Francis Group.

3D slope stability analysis with spatially variable and cross-correlated shear strength parameters

D. Varkey, M.A. Hicks & P.J. Vardon
Section of Geo-Engineering, Faculty of Civil Engineering and Geosciences, Delft University of Technology, Delft, The Netherlands

ABSTRACT: The paper investigates the stability of slopes with spatially variable and cross-correlated shear strength parameters in 3D. The influence of various cross-correlation coefficients between these parameters on the probability of 3D slope failure has been considered for different levels of anisotropy of the heterogeneity in the shear strength. Specifically, 3D random fields of cohesion and friction angle were generated using the Local Average Subdivision method, and these were correlated with each other by various degrees. The fields were then linked to finite element analyses within a Monte Carlo framework. The results indicate that a positive cross-correlation between the parameters reduces the slope reliability, whereas a negative cross-correlation between the parameters increases the reliability.

1 INTRODUCTION

The inherent nature of soil is to be spatially variable (Phoon & Kulhawy 1999). The uncertainty in the spatial variability of parameters arises due to a combination of various geologic, environmental and physiochemical processes. However, quantification of this heterogeneity is not a trivial task and demands extensive field and laboratory tests (Jaksa et al. 1999, de Gast et al. 2017). There can also be other types of uncertainties, such as geometric uncertainty in the form of uncertain soil layer boundaries, or epistemic uncertainties associated with sampling, modeling, and so on. The uncertainty in the spatial variability of the shear strength parameters alone has been considered in this paper.

Conventionally, the stability of slopes is calculated deterministically, i.e., by ignoring the spatial variability in heterogeneity within soil layer(s) and considering the entire slope to be made up of a single or multiple homogeneous layers. The outcome of such an analysis is a single factor of safety (FS), which gives no information about the reliability. Ignoring the heterogeneity within the soil has been shown to have a significant influence on computations of FS (Hicks & Samy 2002, Hicks 2007, Cho 2007, among others) and also on the failure mechanisms (Hicks & Spencer 2010). Various reliability-based methods have been developed to include heterogeneity; for example, the first order second moment method, first order reliability method, point estimate method, stochastic response surface methods and the random finite element method (RFEM) (Fenton & Griffiths 2008). The outcome of RFEM is a range of possible responses of the structure. Research has also been done to efficiently use the available data to condition random fields, for improving the confidence in results (Lloret-Cabot et al. 2012, Li et al. 2016).

Soils generally exhibit spatial variability in a range of parameters. These parameters, in addition to being correlated over certain lengths, may also be correlated to each other. The influence of cross-correlation between effective cohesion (c') and effective friction angle (ϕ') on bearing capacity predictions has been investigated by Cherubini (2000) and Fenton & Griffiths (2003). The influence of this cross-correlation on the reliability of slopes (Le 2014, Javankhoshdel & Bathurst 2016, among others), as well as different methods for constructing the bivariate distributions (Tang et al. 2015) and their influence on the reliability of retaining walls (Li et al. 2015) have also been investigated. Griffiths et al. (2009a) identified critical values of the coefficients of variation of the shear strength parameters, beyond which ignoring the spatial variability gives unconservative results with or without cross-correlation between them.

Research has also been done on the reliability analysis of slopes in 2D to understand the influence of various levels of heterogeneity in the mechanical and hydraulic parameters (Arnold & Hicks 2011), and on making use of inverse analysis techniques to reduce the uncertainty in hydraulic conductivity by using pore pressure measurements (Vardon et al. 2016). All these studies are based on the assumption that the mechanical and hydraulic parameters are correlated over an infinite distance in the third dimension. Although this is generally not the case, only a limited amount of research has been done regarding full 3D probabilistic analysis, possibly due to the large computational requirements.

Vanmarcke (1977) pioneered 3D reliability assessments of slopes by assuming the governing soil parameter to be the spatial average of the randomly varying parameter over a predefined surface. In contrast, 3D RFEM does not make any assumption regarding equivalent soil parameter or failure mechanism, although it requires a large computational effort to carry out multiple realisations. Spencer (2007), Griffiths et al. (2009b), Hicks & Spencer (2010) and Li et al. (2015) used 3D RFEM to investigate the influence of anisotropy of the heterogeneity in undrained shear strength and slope length in the third dimension on the estimation of failure probability. Hicks & Spencer (2010) grouped the failure modes into three different categories based on the anisotropy of the heterogeneity in shear strength relative to the slope dimensions. Strategies for quantification of the failure consequences have also been developed (Hicks et al. 2008, Huang et al. 2013, Hicks et al. 2014).

This paper considers the spatial variability and cross-correlation between shear strength parameters (c' and ϕ') for an idealised long slope. The random fields of the parameters were generated using the 3D Local Average Subdivision method, and linked with the finite element model within a Monte Carlo framework. Different values of anisotropy of the heterogeneity in the shear strength were considered. The influence of different cross-correlation coefficients between these parameters on the probability of failure of a 3D slope has been investigated.

2 RANDOM FINITE ELEMENT METHOD (RFEM)

The mathematical representation of the spatial variability of soil parameters can be made in the form of a random field. This can be univariate or multivariate, depending whether the field value at a point in space is a random variable or a random vector. The field is said to be stationary if the mean (μ) and variance (σ^2) of the random variables are constant and the autocorrelation coefficient (ρ) is only dependent on the separation between the points (t, t') under consideration. The correlation structure for the random variable (X) between these points is given as:

$$\rho(X_t, X_{t'}) = \frac{\mathrm{E}\left[(X_t - \mathrm{E}[X_t])(X_{t'} - \mathrm{E}[X_{t'}])\right]}{\sigma_t \sigma_{t'}} \tag{1}$$

where X_t and $X_{t'}$ are the respective values of X at t and t', and $\mathrm{E}[X_t]$, $\mathrm{E}[X_{t'}]$ and σ_t, $\sigma_{t'}$ are the expectations and standard deviations of X, respectively. For a stationary random field, $\mathrm{E}[X_t] = \mathrm{E}[X_{t'}] = \mu$ and $\sigma_t \sigma_{t'} = \sigma^2$.

In the context of finite element analysis, the mechanical response of a system is approximated by the spatial discretization of the geometry. RFEM combines random fields with finite elements and hence discretization of the random fields is required, as carried out in this paper by Local Average Subdivision (LAS) (Fenton & Vanmarcke 1990). In this method, a local integral process is obtained by integrating X over a moving window (T), such that the new process has the same average as X and is smoother than X, i.e. with a reduced variance to account for local averaging. The variance reduction ($\Gamma(T)$) is dependent on the correlation function ($\rho(\tau)$) for a stationary process, and is given in 1D as:

$$\Gamma(T) = \frac{2}{T}\int_0^T \rho(\tau)d\tau - \frac{2}{T^2}\int_0^T \tau\rho(\tau)d\tau \tag{2}$$

where τ is the lag distance. A 3D separable Gauss Markov correlation structure is used in this paper, with the correlation in the vertical (z) direction separated from the two horizontal (x and y) directions. The 3D covariance function ($\beta = \sigma^2\rho$) is:

$$\beta(\tau_x, \tau_y, \tau_z) = \sigma^2 \exp\left(-\frac{2\tau_z}{\theta_z} - \sqrt{\left(\frac{2\tau_x}{\theta_x}\right)^2 + \left(\frac{2\tau_y}{\theta_y}\right)^2}\right) \tag{3}$$

where θ_x, θ_y and θ_z are the scales of fluctuation and τ_x, τ_y and τ_z are the lag distances in the respective directions.

The separation of the vertical correlation structure from the two horizontal directions was done to model the long-term depositional characteristic in the soil. It is assumed that the horizontal layers were deposited at the same instant, whereas the vertical deposition occurs over time.

LAS is a top-down recursive approach, which begins with generating a random number (from a standard Gaussian distribution) which is assigned as the initial global mean for the entire domain. Proceeding downwards, the domain is subdivided into equal halves in each direction, i.e. each cell is divided into 2^3 cells at each subdivision level in 3D LAS. In the subdivision process, the global average is preserved by the top-down approach, whereas the variance of the local average reduces and tends towards the target variance as the number of subdivision levels increases. In this paper, the minimum required subdivision level is determined in order to have a variance reduction value not less than 0.8, i.e. as given by the scale of fluctuation of the process being at least four times the averaging window in the last sub-division level (Li 2017).

2.1 *Cross-correlation between variables*

The generated random fields, for say n parameters, can be correlated to each other by using the correlation matrix (R) given in Equation 4, with $\rho_{X_iX_j}$ being the correlation coefficient between the randomly varying parameters, X_i and X_j, at the same point in space.

$$R = \begin{bmatrix} 1 & \rho_{X_1X_2} & .. & \rho_{X_1X_n} \\ \rho_{X_2X_1} & 1 & .. & \rho_{X_2X_n} \\ .. & .. & .. & .. \\ \rho_{X_nX_1} & \rho_{X_nX_2} & .. & 1 \end{bmatrix} \tag{4}$$

The generated n univariate Gaussian random variables are cross-correlated by using the Cholesky decomposition (LL^{T}) of R, and using the following matrix transformation to generate the cross-correlated fields (ζ_i):

$$\begin{pmatrix} \zeta_1 \\ .. \\ .. \\ \zeta_n \end{pmatrix} = L \begin{pmatrix} X_1 \\ .. \\ .. \\ X_n \end{pmatrix} \tag{5}$$

where L is the lower triangular matrix. The above transformation requires that the individual random fields are stationary, and the Cholesky decomposition fails if R has negative eigenvalues. Figure 1 shows the random variables for two parameters, X_1 and X_2, correlated to each other with different values of $\rho_{X_1X_2}$.

Figure 2 shows the covariance structure obtained in the field of X_2 cross-correlated to X_1 for different values of $\rho_{X_1X_2}$. The generated fields coincide with the exact covariance structure (Eq. 3) for an isotropic field with $\theta = 1\,\mathrm{m}$. Hence, cross-correlation does not affect the covariance structure within the fields.

Note that for generating anisotropic random fields, the authors have first generated isotropic random fields for each uncertain parameter by LAS using $\theta = \theta_x = \theta_y = \theta_z$ in Equation 3, followed by cross-correlating the fields using Equation 5. This field was then post-processed by squashing and/or stretching in the respective directions to generate the required level of anisotropy ($\xi = \theta_{\mathrm{h}}/\theta_{\mathrm{v}}$); see Hicks & Samy (2002) and Hicks & Spencer (2010) for details. The cross-correlated random fields corresponding to each parameter were then transformed into their physical space using the point statistics and type of parameter distribution.

3 PROBLEM DESCRIPTION

A 50 m long slope, with the cross-sectional geometry shown in Figure 3, was analysed by RFEM. Different values of the cross-correlation coefficient ($\rho_{c'\phi'}$) between the shear strength parameters (c' and ϕ') were considered. The parameters of the model are summarised in Table 1. The slope was meshed with a total of 4000 20-node regular hexahedral elements with a $2 \times 2 \times 2$ Gaussian integration scheme. The elements were of size $1\,\mathrm{m} \times 1\,\mathrm{m}$ in plan and $0.5\,\mathrm{m}$ in depth. The boundary conditions applied to the model were: fixed along the base, rollers on the side face, and rollers on the vertical end-faces allowing only vertical movement; see Spencer (2007) for an explanation of these boundary conditions. The random field variables corresponding to each uncertain parameter, after post-processing, were assigned to the Gauss points within each element. A linear elastic, perfectly plastic Mohr-Coulomb model was used to define the stress-strain conditions within the problem domain. In each realisation, the in-situ stresses were generated by apply-

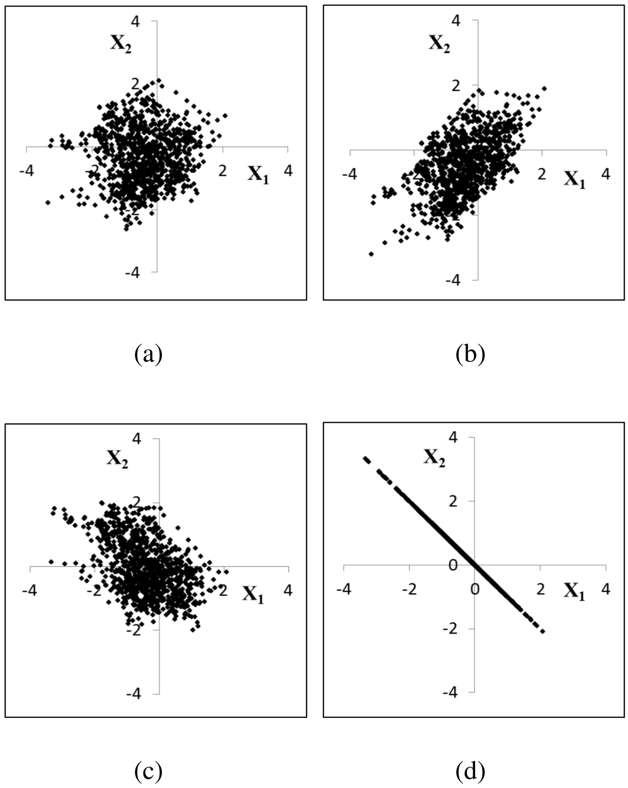

Figure 1: Cross-correlated fields in standard normal space; (a) $\rho_{X_1X_2} = 0$, (b) $\rho_{X_1X_2} = 0.5$, (c) $\rho_{X_1X_2} = -0.5$, (d) $\rho_{X_1X_2} = -1$

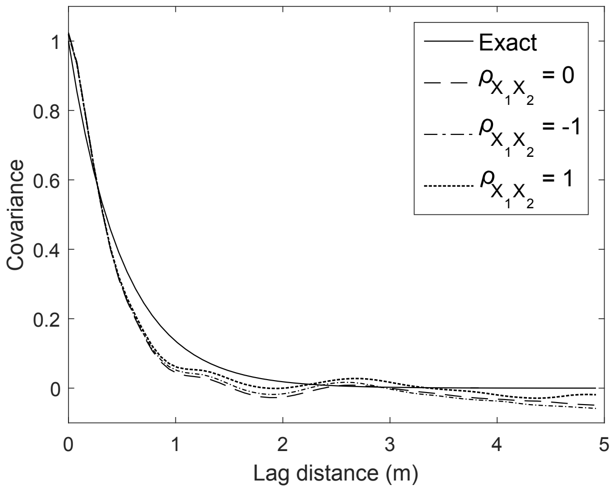

Figure 2: Covariance structure obtained in a cross-correlated isotropic 3D field with $\theta = 1\,\mathrm{m}$ and domain side length of $5\,\mathrm{m}$, for different cross-correlation coefficients ($\rho_{X_1X_2}$)

Table 1: List of parameter values

Parameter	Mean	Standard deviation
Cohesion	10 kPa	2 kPa
Friction angle	25°	5°
Dilation angle	0°	-
Young's modulus	1×10^5 kPa	-
Poisson's ratio	0.3	-
Unit weight	20 kN/m^3	-

ing gravity loading in a single step, and the slope was checked for stability under its own weight using the strength-reduction method. A total of 500 realisations were carried out for each set of statistics of the parameters, and a distribution of the FS was determined.

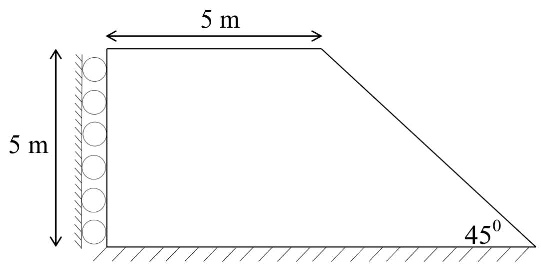

Figure 3: Sketch of the cross-sectional geometry

A wide range of values for the cross-correlation coefficient between c' and ϕ' have been reported in the literature. The different values of $\rho_{c'\phi'}$ are attributed to different soil types, sampling techniques and testing rates used. The results for different values of $\rho_{c'\phi'}$ are summarised in the next section.

4 RESULTS

In this section, the response of the structure, in terms of FS distributions obtained from 500 realisations of the problem by RFEM, are presented. For simplicity, the same value of ξ was used to generate the random fields for c' and ϕ'. The vertical scale of fluctuation θ_v was fixed to 1m in all the analyses. A 2D deterministic analysis of the slope for the mean values given in Table 1 gave a FS of 1.4.

Figure 4 plots the FS obtained in each realisation using perfectly positive and perfectly negative cross-correlated c'-ϕ' fields, against the FS obtained from uncorrelated c'-ϕ' fields for $\theta_\mathrm{h} = 12$ m. Extreme values of $\rho_{c'\phi'}$ compared to values reported in literature have been chosen, to highlight the differences between the solutions. For positively cross-correlated fields of the shear strength parameters, the weak zones (and the strong zones) of the shear strength are exaggerated compared to uncorrelated fields, making it easier to seek out the failure path. Hence, the positive cross-correlation decreases (or increases) the safety factor for each realisation and increases the range of possible solutions. In contrast, a negative cross-correlation between the shear strength parameters reduces the range of possible solutions.

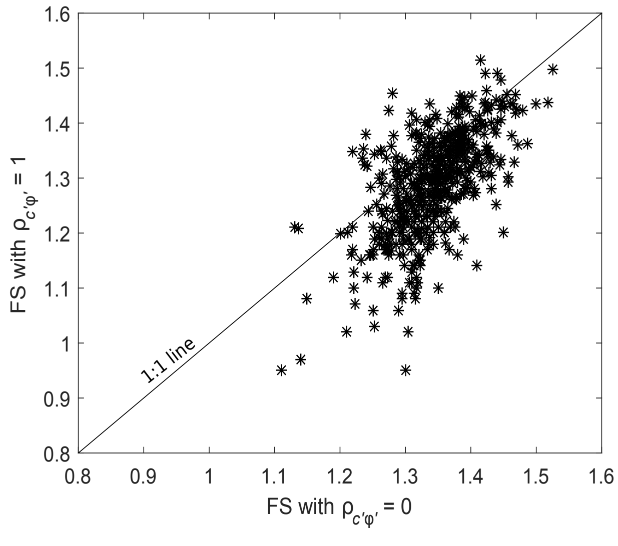

(a)

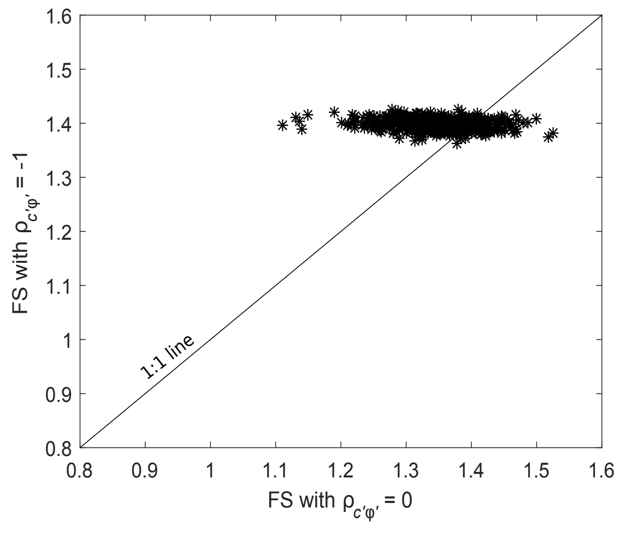

(b)

Figure 4: FS obtained with (a) $\rho_{c'\phi'} = 1$, and (b) $\rho_{c'\phi'} = -1$ against $\rho_{c'\phi'} = 0$ for $\theta_\mathrm{h} = 12$ m

Figure 5 compares the distributions of FS at different values of ξ, for different $\rho_{c'\phi'}$. The different values of ξ considered in Figure 5(a-c) are similar to deterministic, 3D stochastic and 2D stochastic solutions, respectively, as in Hicks & Spencer (2010) and Varkey et al. (2017). In Figure 5(b), for the case of $\xi = 12$, i.e., for a value of θ_h lying between the slope height and half of the slope length, there is the possibility of discrete weak zones generated within each realisation (Spencer 2007, Varkey et al. 2017). This results in the mean FS being lower than 1.4, which is also the case for other values of θ_h lying in this range (not shown in Fig. 5). For positive values of $\rho_{c'\phi'}$, the failure propagates through even weaker zones and the mean FS reduces further below 1.4. In contrast, for negatively cross-correlated fields of c' and ϕ', the average of the mobilised shear strength over all the realisations increases. This results in the mean FS tending towards the deterministic FS for $\rho_{c'\phi'} = -1$. Also,

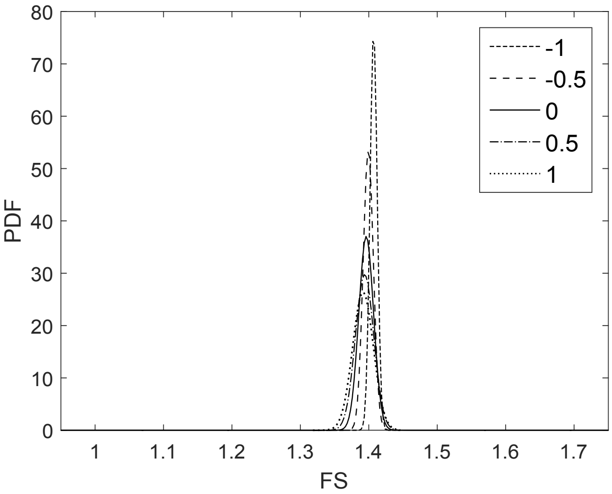

(a)

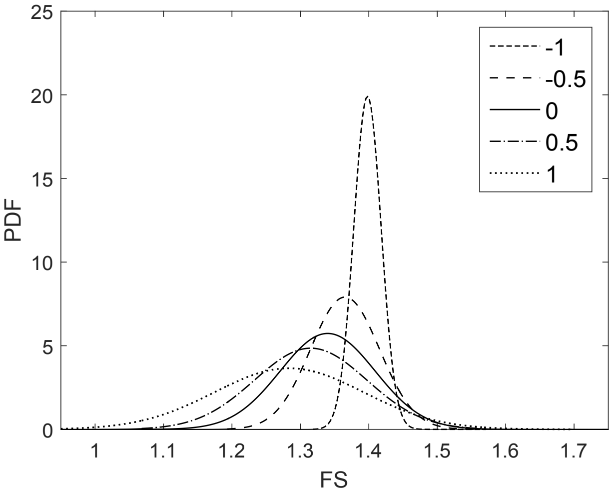

(b)

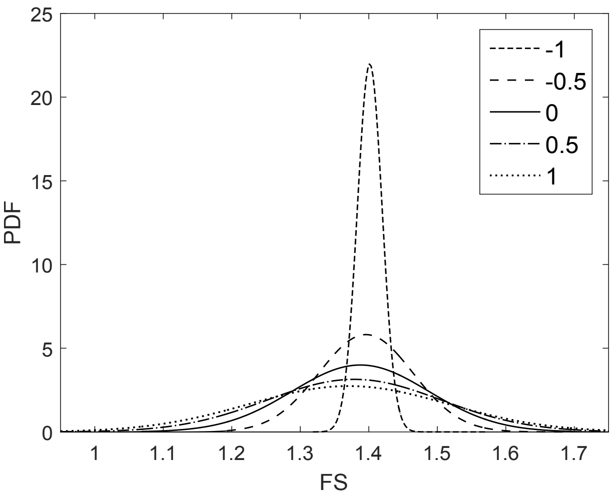

(c)

Figure 5: Probability density functions of FS for different values of $\rho_{c'\phi'}$; (a) $\xi = 1$, (b) $\xi = 12$, (c) $\xi = 2000$

the range of possible solutions decreases considerably compared to the uncorrelated and positively cross-correlated fields, and the variance of FS therefore reduces considerably.

For the case of a very large θ_{h} relative to the slope length (Fig. 5(c)), there is a wide range of possible solutions for uncorrelated fields and an even wider range for positively correlated fields. This wide range is due to the relative locations of very extensive weak zones through which the failure propagates.

For very small scales of fluctuation relative to the slope height, as in Figure 5(a), extreme averaging takes place and thus there is a negligible difference between the responses with different values of $\rho_{c'\phi'}$.

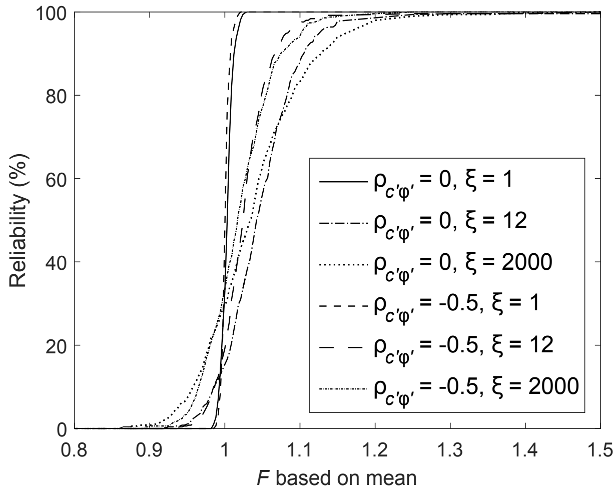

(a)

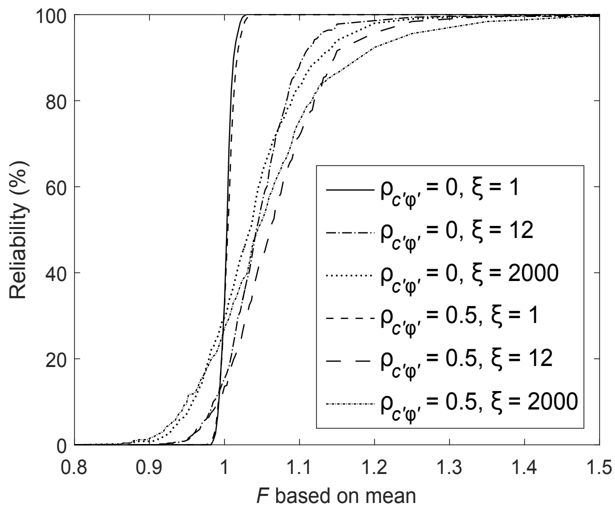

(b)

Figure 6: Reliability of the slope for various values of anisotropy of the heterogeneity (ξ) in the shear strength; (a) $-0.5 \leq \rho_{c'\phi'} \leq 0$, (b) $0 \leq \rho_{c'\phi'} \leq 0.5$

Figure 6 shows the reliability obtained at different values of F for slopes with $\rho_{c'\phi'} = -0.5$, 0 and 0.5, for the range of ξ values considered in Figure 5. Here, F is defined as the factor of safety based only on the mean shear strength. The reliability at each F for a given set of input statistics is calculated as:

$$\text{Reliability} = 1 - \frac{N_{\mathrm{f}}}{N} \tag{6}$$

where N is the total number of realisations and N_f is the number of realisations in which the slope fails at a value less than or equal to F.

A negative cross-correlation between c' and ϕ' increases the reliability, whereas a positive cross-correlation decreases the reliability of the structure for all values of ξ considered.

5 CONCLUSIONS

An idealised 50m long slope has been analysed by RFEM for various degrees of cross-correlation between the shear strength parameters (c' and ϕ'). It has been shown that assuming a positive cross-correlation between the parameters reduces the reliability, whereas a negative cross-correlation between the parameters increases the reliability of the slope. At intermediate and very large horizontal scales of fluctuation of c' and ϕ', assuming a perfectly negative cross-correlation considerably reduces the range of possible outcomes and makes the mean safety factor tend towards the plane strain safety factor based on the mean values alone. Hence, caution is needed when assigning cross-correlation coefficients between the shear strength parameters in an analysis.

ACKNOWLEDGEMENT

This work is part of the research programme Reliable Dykes with project number 13864 which is financed by the Netherlands Organisation for Scientific Research (NWO), and was carried out on the Dutch National e-infrastructure with the support of SURF Foundation.

REFERENCES

Arnold, P. & M. A. Hicks (2011). A stochastic approach to rainfall-induced slope failure. In *Proc. 3rd Int. Symp. Safety and Risk*, Munich, pp. 107–115.

Cherubini, C. (2000). Reliability evaluation of shallow foundation bearing capacity on c', ϕ' soils. *Canadian Geotech. J. 37*, 264–269.

Cho, S. E. (2007). Effects of spatial variability of soil properties on slope stability. *Engng. Geology 92*(3), 97–109.

de Gast, T., P. J. Vardon, & M. A. Hicks (2017). Estimating spatial correlations under man-made structures on soft soils. In *Proc. 6th Int. Symp. Geotech. Safety and Risk*, Colorado, USA, pp. 382–389.

Fenton, G. A. & D. V. Griffiths (2003). Bearing-capacity prediction of spatially random c-ϕ soils. *Canadian Geotech. J. 40*, 54–65.

Fenton, G. A. & D. V. Griffiths (2008). *Risk Assessment in Geotechnical Engineering*. John Wiley & Sons.

Fenton, G. A. & E. H. Vanmarcke (1990). Simulation of random fields via local average subdivision. *J. Engng. Mech. 116*(8), 1733–1749.

Griffiths, D. V., J. Huang, & G. A. Fenton (2009a). Influence of spatial variability on slope reliability using 2D random fields. *J. Geotech. Geoenviron. Engng. 135*(10), 1367–1378.

Griffiths, D. V., J. Huang, & G. A. Fenton (2009b). On the reliability of earth slopes in three dimensions. *Proc. R. Soc. London A: Math., Phys. Engng. Sc. 465*, 3145–3164.

Hicks, M. A. (2007). *Risk and Variability in Geotechnical Engineering*. Thomas Telford.

Hicks, M. A., J. Chen, & W. A. Spencer (2008). Influence of spatial variability on 3D slope failures. In *Proc. 6th Int. Conf. Computer Simulation Risk Analysis and Hazard Mitigation*, Kefalonia, pp. 335–342.

Hicks, M. A., J. D. Nuttall, & J. Chen (2014). Influence of heterogeneity on 3D slope reliability and failure consequence. *Comp. Geotech. 61*, 198–208.

Hicks, M. A. & K. Samy (2002). Influence of heterogeneity on undrained clay slope stability. *Quart. J. Engng. Geology and Hydrogeology 35*(1), 41–49.

Hicks, M. A. & W. A. Spencer (2010). Influence of heterogeneity on the reliability and failure of a long 3D slope. *Comp. Geotech. 37*(7), 948–955.

Huang, J., A. V. Lyamin, D. V. Griffiths, K. Krabbenhoft, & S. Sloan (2013). Quantitative risk assessment of landslide by limit analysis and random fields. *Comp. Geotech. 53*, 60–67.

Jaksa, M., W. Kaggwa, & P. Brooker (1999). Experimental evaluation of the scale of fluctuation of a stiff clay. In *Proc. 8th Int. Conf. Appl. Statistics and Probability in Civil Engng.*, Sydney, pp. 415–422.

Javankhoshdel, S. & R. J. Bathurst (2016). Influence of cross-correlation between soil parameters on probability of failure of simple cohesive and c-ϕ slopes. *Canadian Geotech. J. 53*(5), 839–853.

Le, T. M. H. (2014). Reliability of heterogeneous slopes with cross-correlated shear strength parameters. *Georisk: Assessment and Management of Risk for Engineered Systems and Geohazards 8*(4), 250–257.

Li, D.-Q., L. Zhang, X.-S. Tang, W. Zhou, J.-H. Li, C.-B. Zhou, & K.-K. Phoon (2015). Bivariate distribution of shear strength parameters using copulas and its impact on geotechnical system reliability. *Comp. Geotech. 68*, 184–195.

Li, Y. (2017). *Reliability of long heterogeneous slopes in 3D*. Ph.D. thesis, Delft University of Technology, The Netherlands.

Li, Y., M. A. Hicks, & J. D. Nuttall (2015). Comparative analyses of slope reliability in 3D. *Engng. Geology 196*, 12–23.

Li, Y., M. A. Hicks, & P. J. Vardon (2016). Uncertainty reduction and sampling efficiency in slope designs using 3D conditional random fields. *Comp. Geotech. 79*, 159–172.

Lloret-Cabot, M., M. A. Hicks, & A. P. van den Eijnden (2012). Investigation of the reduction in uncertainty due to soil variability when conditioning a random field using Kriging. *Géotechnique Letters 2*(3), 123–127.

Phoon, K.-K. & F. H. Kulhawy (1999). Characterization of geotechnical variability. *Canadian Geotech. J. 36*(4), 612–624.

Spencer, W. A. (2007). *Parallel stochastic and finite element modelling of clay slope stability in 3D*. Ph.D. thesis, University of Manchester, UK.

Tang, X.-S., D.-Q. Li, C.-B. Zhou, & K.-K. Phoon (2015). Copula-based approaches for evaluating slope reliability under incomplete probability information. *Struct. Safety 52*, 90–99.

Vanmarcke, E. H. (1977). Reliability of earth slopes. *J. Geotech. Engng Div. 103*(11), 1247–1265.

Vardon, P. J., K. Liu, & M. A. Hicks (2016). Reduction of slope stability uncertainty based on hydraulic measurement via inverse analysis. *Georisk: Assessment and Management of Risk for Engineered Systems and Geohazards 10*(3), 223–240.

Varkey, D., M. A. Hicks, & P. J. Vardon (2017). Influence of spatial variability of shear strength parameters on 3D slope reliability and comparison of analysis methods. In *Proc. 6th Int. Symp. Geotech. Safety and Risk*, Colorado, USA, pp. 400–409.